Appl Phys B (2009) 95: 261–268
DOI 10.1007/s00340-009-3448-5

Applied Physics B
Lasers and Optics

Spatial photorefractive solitons with picosecond laser pulses

J. Imbrock · C. Heese · C. Denz

Received: 1 December 2008 / Revised version: 16 February 2009 / Published online: 27 February 2009

Abstract We report on the formation of spatial optical solitons in photorefractive media using picosecond laser pulses. Solitons are generated with laser pulses in the visible and infrared wavelength region using photorefractive strontium barium niobate. The dynamics of the soliton formation and the region of existence is studied in detail.

PACS 42.65.Tg · 42.65.Hw · 42.70.Nq

1 Introduction

Optical solitons have been an active area of research since more than two decades due to their simultaneous importance for basic soliton research as well as applications in optical information processing. An optical soliton can be formed while a beam is propagating through a material when the dispersion of the material is compensated for by a nonlinearity. Typically, the field is divided into spatial optical solitons, where the dispersion is given by diffraction, and temporal solitons, short pulses where dispersion of the group velocity is acting [1, 2]. Combining these two fields leads to the exciting and highly actual field of optical solitons that are stable in space and time, so called spatio-temporal solitons or "light bullets" [3, 4]. Despite many theoretical approaches (see e.g. [4]), spatio-temporal solitons that are stable in all three spatial dimensions as well as in the time domain have not yet been experimentally realized. Several attempts however have already shown spatio-temporal solitons in reduced dimensions [5]. Beneath the concept of guiding and confining temporal solitons in space (see e.g. [6, 7]), it is also of interest to investigate the propagation of ultra short laser pulses in materials that allow for creation of spatial optical solitons.

For this purpose, in this paper we investigate the propagation of ultra short laser pulses in photorefractive media. Since the first observation of photorefractive screening solitons by Segev et al. [8], a variety of general basic phenomena related to the propagation of optical solitons in photorefractive media have been investigated (see e.g. [9]). Among them are incoherent solitons [10–12], vector solitons [13–15], arrays of solitons [16], soliton interaction [17–19] and their control, to name here a few of them. Almost all of these experiments have been performed with cw-laser light, and not much is known about the formation of photorefractive solitons with laser pulses. Immediately the question arises if a spatial soliton can be formed with short laser pulses and if it might be possible to build up a soliton with just one pulse due to the high peak intensity. For instance, in strontium barium niobate (SBN), it has been reported that solitons can be formed with a few nanosecond laser pulses of high intensity in the green wavelength region [20].

A spatial photorefractive screening soliton is generated by launching a focused laser beam or pulse into a crystal that is biased by an external applied electrical field along the c-axis. In the illuminated region light can excite electrons which can drift in the electrical field and are finally trapped in dark regions. The internal field will lower the applied field leading to a refractive index change via the electro-optic effect. To prevent the total screening of the applied field it is necessary to illuminate the crystal homogeneously. By this

J. Imbrock · C. Heese · C. Denz (✉)
Institut für Angewandte Physik and Center for Nonlinear Science, Westfälische Wilhelms-Universität, 48149 Münster, Germany
e-mail: denz@uni-muenster.de

C. Heese
Institute for Quantum Electronics, ETH Zürich, 8093 Zürich, Switzerland

background illumination the light-induced refractive index change will saturate for large intensities. Depending on the relative intensity of the beam to the background there exists a dynamic equilibrium leading to a steady-state lensing effect. The speed of soliton formation depends on the photorefractive response time and therefore on the light intensity. The soliton formation with cw-laser light can be different from that with laser pulses because of a different light-induced charge transport process at high and low intensities [21].

Solitons can exist in a certain parameter range depending on the spatial width of the beam or pulse, the material response, the applied voltage, and the soliton and background intensity. To describe the propagation of an extraordinarily polarized beam or pulse in a photorefractive crystal like SBN, one can employ the generalized nonlinear Schrödinger equation,

$$i\frac{\partial E}{\partial z} + \nabla^2 E + \Delta n(I)E = 0, \tag{1}$$

where $I = |E|^2$ is the light intensity. Here, the pulse propagates along the z-axis and the c-axis of the crystals is orientated along the x-axis. The nonlinear contribution to the refractive index is given by

$$\Delta n(I) = \Gamma \frac{\partial \varphi}{\partial x}, \tag{2}$$

where $\Gamma = k^2 n_0^2 r_{33} E_{\text{ext}}$ is defined through the electro-optic coefficient r_{33}, the externally applied electric field E_{ext}, and $k = 2\pi n_0/\lambda$ with the unperturbed refractive index n_0 at the wavelength λ. The electro-optic coefficient of $Sr_{0.6}Ba_{0.4}Nb_2O_6$ for light that is polarized extraordinarily (parallel to the c-axis) ($r_{33} \approx 235$ pm/V) is about five times larger than the coefficient for ordinarily (perpendicular to the c-axis) polarized light ($r_{13} \approx 47$ pm/V). The electrostatic potential of the optically induced space charge field pattern satisfies the equation [22]

$$\nabla^2 \varphi + \nabla\varphi \nabla \ln(1+I) = \frac{\partial}{\partial x} \ln(1+I)\,, \tag{3}$$

where the gradient operator is $\nabla^2 = \partial^2/\partial x^2 + \partial^2/\partial y^2$ and the intensity I is the ratio of the signal or soliton intensity I_{sig} to the background intensity I_{back}.

Assuming an isotropic approximation and neglecting the diffusion of electrons one gets for moderate light intensities in the mW/cm^2 to kW/cm^2 range a saturable refractive index change [21]:

$$\Delta n(I) = -\frac{1}{2} n_0^3 r_{33} \frac{E_{\text{ext}}}{1 + I(x)}. \tag{4}$$

In contrast, at high light intensities in the MW/cm^2 to GW/cm^2 range, the saturation behavior of the refractive index change can be different due to a very large concentration of photoexcited electrons [20, 21]:

$$\Delta n(I) = -\frac{1}{2} n_0^3 r_{33} \frac{E_{\text{ext}}}{\sqrt{(1+I)}}. \tag{5}$$

Considering this nonlinearity in the high-intensity regime one-dimensional photorefractive screening solitons obey the wave equation [21]:

$$\frac{\partial^2 u}{\partial x^2} + \delta\Gamma u - \Gamma \frac{u}{\sqrt{1+u^2}} = 0, \tag{6}$$

with the normalized soliton amplitude $u = E/\sqrt{I_{\text{back}}}$, $\delta = 2[(u_0^2+1)^{1/2} - 1]/u_0^2$, and $u_0 = u(x=0)$. To obtain the spatial profile of the soliton in dependence of intensity one can integrate (6) numerically.

We examine the formation of photorefractive screening solitons in SBN using visible and also infrared picosecond laser pulses. The experimental setup with the laser system and the crystal used is described in the following section. The main results are related to the dynamics of the soliton formation with pulses in the green wavelength region and the region where solitons exists. One crucial parameter in pulse laser experiments that determines the existence of solitons is the time delay between the soliton pulse and the background pulse. This time delay has no counterpart in cw-laser experiments and it turns out that for the existence of solitons the delay between the two pulses should not exceed a certain value depending on the material used. Finally, we demonstrate the generation of solitons with infrared laser pulses that gives the promising perspective to observe solitons using even longer wavelengths, e.g. in the telecommunication wavelength range.

2 Experimental system

The ultra short laser pulses are generated by a laser system consisting of a mode-locked Ti:sapphire oscillator, a regenerative amplifier and an optical parametric amplifier (OPA). The oscillator delivers pulses with a pulse duration of about $\tau_p = 120$ fs, a wavelength of 800 nm, and a repetition rate of 80 MHz. The average power is about 300 mW. The pulses are amplified in a Ti:sapphire regenerative amplifier that is pumped by a nanosecond pulse laser. The regenerative amplifier can deliver either picosecond pulses ($\tau_p = 1.6$ ps) or femtosecond pulses ($\tau_p = 120$ fs) with a repetition rate of 1 kHz and pulse energies of up to 1 mJ. To obtain pulses with wavelengths between 470 nm and 2700 nm an OPA is pumped with the pulses of the regenerative amplifier. First we have examined the formation of solitons with green ($\lambda = 532$ nm) picosecond pulses of the OPA and for the infrared solitons we have used directly the output of the regenerative amplifier ($\lambda = 800$ nm).

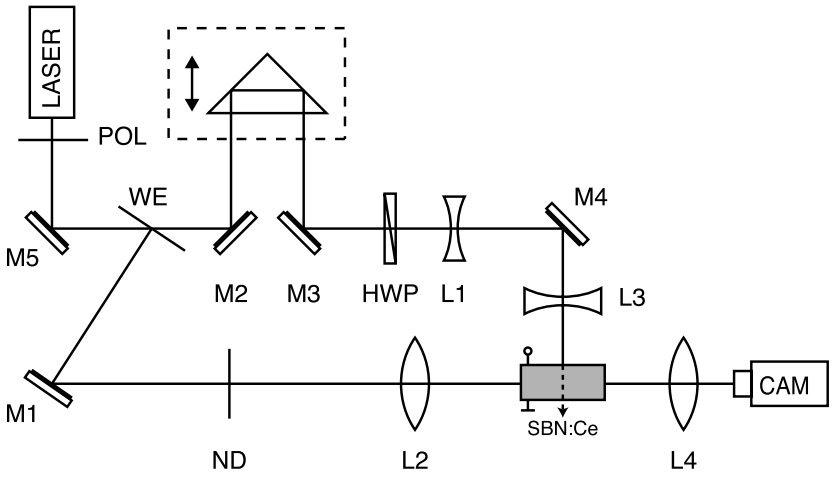

Fig. 1 Experimental setup to create spatial solitons with ultra short laser pulses. Pol: polarizer, WE: wedge, M: mirrors, HWP: half wave plate, ND: neutral density filter, L1 and L4: convex lenses, L2 and L3: concave lenses, CAM: CCD camera

The experimental setup is depicted in Fig. 1. The pulses are divided at a wedge (WE) into two parts. The signal or soliton pulse is focused with a lens (L2) onto the front face of the crystal starting with a beam width of approximately 14 µm. The $Sr_{0.6}Ba_{0.4}Nb_2O_6$ crystal is doped with 0.002 wt.% CeO_2 and its dimensions are $(5 \times 5 \times 20)$ mm. The pulse is propagating along the long z-axis and the c-axis of the crystal is orientated along one of the short axes. The crystal is biased by an external electric field that is applied along the c-axis. The soliton pulse is extraordinarily polarized to use the largest electro-optic coefficient. The front and the back side of the crystal can be imaged onto a CCD camera adjusting lens L4. One background pulse can be delayed with respect to the soliton pulse and is expanded with two convex lenses (L1, L3) to an elliptical pulse. The area of the background pulse is larger than the area of the side faces of the crystal (20 mm × 5 mm). To prevent interference between the soliton and background pulse the latter one is polarized ordinarily by means of a half wave plate. When the soliton intensity I_{sig} is comparable with the background intensity I_{back} a Gaussian beam can converge to a soliton. To get equal intensities, it is necessary to launch most of the pulse energy into the background pulse because the ratio between the two illuminated areas is about $A_{sig}/A_{back} \approx 143\ \mu m^2/1\ cm^2 = 1.42 \times 10^{-6}$. Therefore, the energy of the background pulse is kept fixed at 23 µJ, while the energy of the soliton pulse can be increased up to 0.033 nJ. The peak intensities are on the order of several MW/cm^2.

3 Picosecond solitons with laser pulses in the green wavelength range

First, we try to generate spatial solitons with laser pulses at a wavelength of $\lambda = 532$ nm by using a continuous, incoherent, white light background illumination of a halogen lamp. Here, the intensity of the background light is comparable with typical cw-laser experiments and it is on the order of mW/cm^2. In this experiment, we have varied the soliton energy between 0.001 and 1000 nJ, the applied electrical field between 100 V/cm and 1 kV/cm, and the background intensity was varied continuously. We found that it is not possible to generate solitons with ultra short laser pulses and continuous white light background illumination. At low pulse energies, self-focusing cannot be observed, whereas at high intensities the pulse breaks up into filaments. Therefore, the following measurements have been carried out with a pulsed background illumination as shown in Fig. 1.

We employed a signal-to-background intensity ratio of about $I_{sig}/I_{back} = 1$. The input pulse is focused to a beam diameter of $w_0 = 11$ µm and the background energy density is $E_{back} = 24$ µJ/cm^2. By varying the electrical field a soliton state can be reached. Figure 2(a) shows the pulse at the front of the crystal, and Fig. 2(b) shows the diffracted output in the linear case without applied electrical field. With an applied electrical field of $E_{ext} = 1$ kV/cm, the diffraction is compensated for by the nonlinearity and after some typical formation time a spatial optical soliton builds up. The profile of the soliton in steady state can be seen in Fig. 2(c).

3.1 Soliton dynamics

The time for the formation of the soliton in Fig. 2(c) is on the order of three minutes considering the measurement time. Taking into account the pulse duration of $\tau_p = 1.6$ ps and the repetition rate of 1 kHz, 3 minutes of measurement time correspond to an illumination time of 288 ns. After this transient formation time, the soliton remains stable. In Fig. 3, the soliton width parallel as well as perpendicular to the applied electrical field is plotted in dependence of the measurement time. The pulse focuses from 230 µm × 330 µm to 23 µm × 20 µm, which is comparable with the input dimensions of 13 µm × 14 µm. In the first seconds after applying

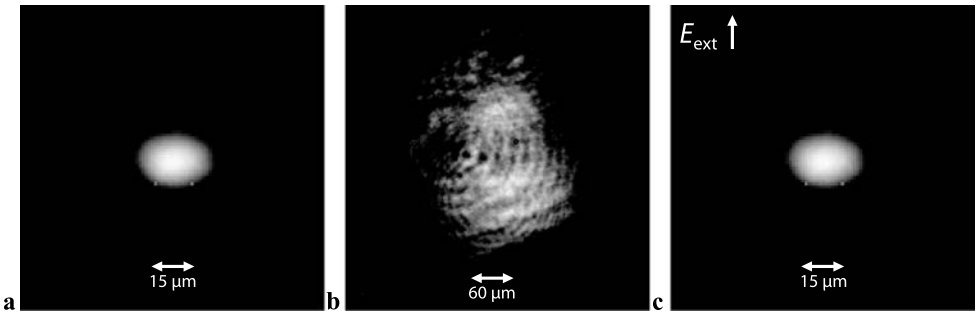

Fig. 2 Pictures of the front and back side of the crystal. (**a**) Focused laser pulse ($\lambda = 532$ nm, $\tau_p = 1.6$ ps) on the front of the crystal, (**b**) diffracted pulse at the back side of the crystal, (**c**) soliton at the back side with an applied electric field $E_{ext} = 1$ kV/cm

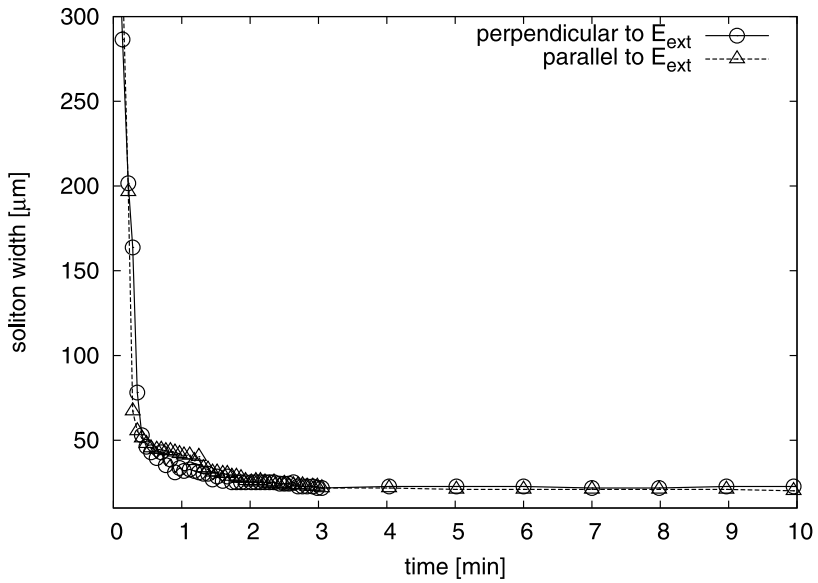

Fig. 3 Spatial width of the soliton pulse in dependence of the measurement time. After applying an electrical field of $E_{ext} = 1$ kV/cm the pulse focuses to a soliton

the electrical field, the soliton bends into the direction of the applied field while the position perpendicular to the c-axis remains constant (Fig. 4). First, the soliton moves 80 µm away from its initial position and settles down 50 µm away. After about three minutes the movement stops completely and the final soliton state is reached. This is similar to the dynamics of cw-soliton formation [23].

3.2 Soliton existence curve

A stable soliton can exist in a certain parameter range depending on the applied electrical field, the signal beam diameter, the signal and background intensity, respectively. We find solitons that are stable in time for an applied electrical field of $E_{ext} = 1$ kV/cm. Therefore, the following experiments have been carried out with this fixed electrical field. By varying the signal intensity the soliton width is measured. With decreasing intensity ratio I_{sig}/I_{back} the soliton width is increasing rapidly as can be seen in Fig. 5. All measurements have been repeated several times and the error bars of the measured soliton widths correspond to the standard deviation. The smallest soliton width is reached at an intensity ratio of approximately $I_{sig}/I_{back} = 2$. Increasing the signal intensity further leads to slightly larger soliton widths. For intensity ratios larger than 20 the solitons are no longer stable, i.e., they break up into filaments. The width of a soliton in the direction of the applied electrical field, i.e. along the c-axis, is slightly larger than the width perpendicular to the c-axis. The solid line in Fig. 5 is obtained by integrating (6) numerically with the experimental parameters $n_0 = 2.35$, $r_{33} = 235$ pm/V, $\lambda = 532$ nm, and $E_{ext} = 1$ kV/cm.

3.3 Influence of the pulse delay

The experiments so far have been achieved with signal and background pulses that overlap in time simultaneously. In the following, we delay the signal pulse with respect to the background pulse. When the soliton pulse reaches the crystal a few pulse lengths (≈50 ps) before or after the background pulse, the process of soliton formation still looks the same. In Fig. 6 the existence curves for three different delays are shown. The applied electrical field is kept fixed at 1 kV/cm for all measurements. The existence curve for zero delay corresponds to the existence curve in Fig. 5. When the soliton pulse reaches the crystal 2 ns after the background

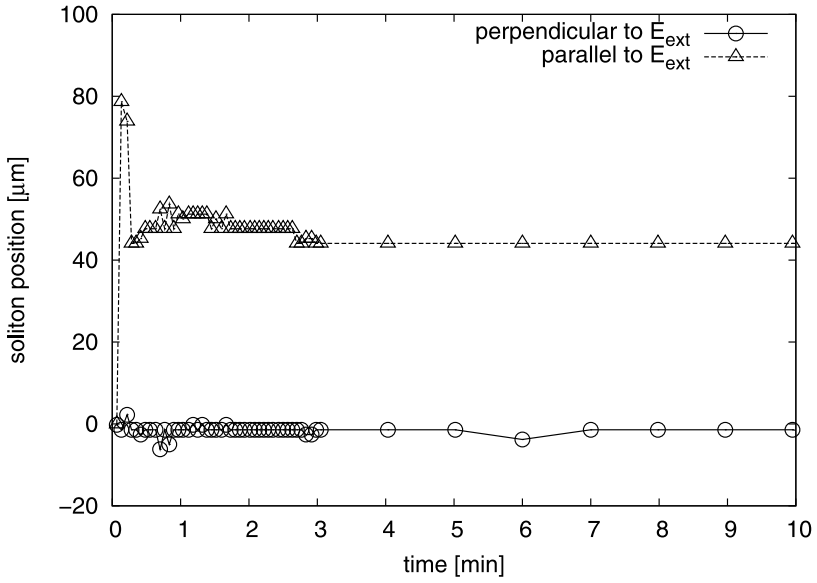

Fig. 4 Time dependence of the soliton position after applying an electrical field of $E_{\text{ext}} = 1$ kV/cm. The pulse bends into the direction of the electric field

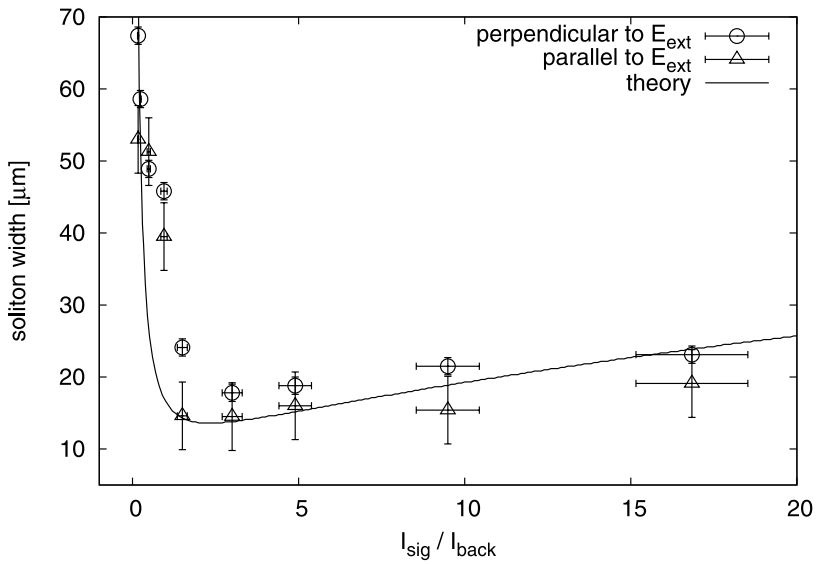

Fig. 5 Existence curve for spatial solitons created with picosecond laser pulses at $\lambda = 532$ nm with an applied electrical field of $E_{\text{ext}} = 1$ kV/cm. The smallest soliton width is reached at $I_{\text{sig}}/I_{\text{back}} \approx 2$. The *solid line* is a numerical integration of the nonlinear wave equation (6)

pulse solitons can still be formed. These solitons remain stable for larger intensity ratios $I_{\text{sig}}/I_{\text{back}}$ in comparison to the measurements with zero delay. Up to a delay of 4 ns stable solitons can be generated. For delays larger than 4 ns the solitons are unstable. However, the strong increase of the soliton width for small intensity ratios cannot be measured for delayed pulses, since stable solitons could not be found experimentally in this intensity region.

4 Picosecond solitons with laser pulses in the infrared wavelength range

Spatial solitons in the infrared wavelength range can be created with the output pulses of the regenerative amplifier at $\lambda = 800$ nm with a pulse width of $\tau_{\text{p}} = 1.6$ ps and a repetition rate of 1 kHz. The experimental setup is the same as for the experiments with laser pulses in the green wavelength region (Fig. 1). First, we have looked for a self-focusing at 800 nm without any background illumination. By applying an electrical field the diffracted pulse focuses to a spot in approximately one minute and then breaks up into filaments. The origin of this self-focusing is due to the photorefractive effect, because the induced refractive index lens is stable in the dark after switching off the applied electrical field and it can be erased with white light. To generate solitons that are stable in time, an infrared background pulse has been used. The existence curve for infrared spatial solitons at $E_{\text{ext}} = 1$ kV/m is depicted in Fig. 7. The soliton width decreases with increasing intensity and reaches a minimum at

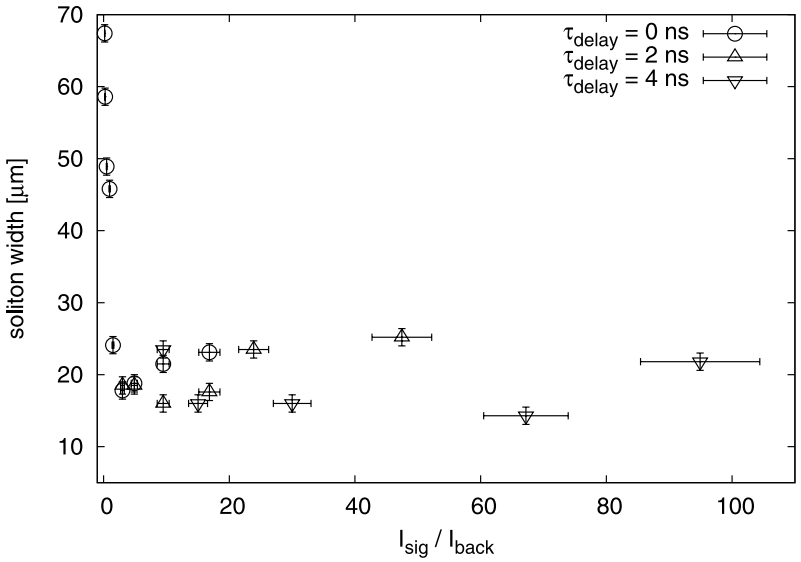

Fig. 6 Soliton width in the direction along the applied electrical field in dependence of the intensity for different time delays between the signal and background pulse ($E_{ext} = 1$ kV/cm, $\lambda = 532$ nm)

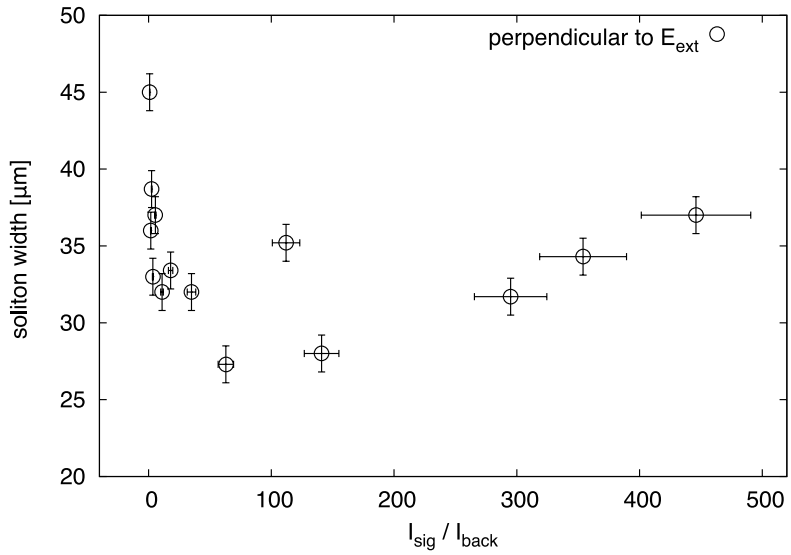

Fig. 7 Existence curve for spatial solitons created with picosecond laser pulses at $\lambda = 800$ nm with an applied electrical field of $E_{ext} = 1000$ V/cm. The smallest soliton width is reached at $I_{sig}/I_{back} \approx 63$

an intensity ratio of approximately 63, which is larger than the minimum of the solitons induced with laser pulses in the green wavelength region (Fig. 5). Increasing the signal intensity further leads to a decrease in the soliton widths. However, even for a very low background illumination, i.e., high soliton intensity, stable solitons can be formed.

5 Discussion

The experimental results reveal that spatial photorefractive screening solitons can be created with ultra short laser pulses. However, a single picosecond pulse cannot form a soliton as the photorefractive response time is much larger than the pulse duration $\tau_p = 1.6$ ps. The photorefractive response time or dielectric relaxation time is the characteristic time to build up a space-charge field, i.e. to create the final refractive index change. The dielectric relaxation time $\tau_d = \epsilon\epsilon_0/\sigma$ depends on the photoconductivity σ, the dielectric constant ϵ, and the permittivity of free space ϵ_0. As the time of self-focusing is on the order of a minute (Fig. 3) the crystal has to be illuminated about 100 ns, taking into account the pulse length $\tau_p = 1.6$ ps and the repetition rate of 1 kHz. Therefore, for pulse intensities of about 35 MW/cm^2, the photorefractive response time τ_d is on the order of 100 ns. Using picosecond pulses the final soliton state will be reached after about 100,000 pulses depending on light intensity. On the other hand, with nanosecond pulses of comparable intensities the final soliton state can be reached after a few pulses [20].

It is essential to use a pulsed background illumination, since the background light induces a photoconductivity that

should be on the same order as the photoconductivity induced by the soliton pulse. One picosecond soliton pulse excites electrons in the illuminated region from Ce^{3+} donors to the conduction band [24]. The excited electrons lead to a photoconductivity that increases linearly with increasing pulse intensity. The lifetime τ_e of the free electrons is on the order of a few nanoseconds [25]. Finally the electrons are trapped in dark regions by Ce^{4+} ions. This means that during one pulse the photoconductivity increases instantaneously and decays to zero after a few nanoseconds. The photoconductivity induced by the background light has to be on the same order as the photoconductivity induced by the soliton pulse. Thus, a continuous white light illumination with intensities of a few mW/cm^2 does not lead to a significant increase in the photoconductivity and a saturable nonlinearity cannot be achieved. In addition a refractive index change will be erased by continuous white light during the time of 1 ms between two pulses.

The experimental results of the build-up of a soliton with laser pulses in the green wavelength region as well as beam bending dynamics and strength are very similar to the formation of spatial solitons with cw-laser light [23]. During the soliton formation the pulse bends into the direction of the applied electrical field due to the diffusion process of the excited electrons. After the beam bending has stopped the final soliton state is reached. The spatial shape of a steady-state soliton is slightly elliptical due to the anisotropy of the nonlinearity. Also, the existence curve of solitons with visible ps-pulses looks very similar to the existence curve of cw-laser solitons [26] as the smallest soliton width is reached at an intensity ratio of about 2. The increase of the soliton width with increasing intensity is not as pronounced as in cw-laser experiments. This can be explained by the high pulse intensities. At high light intensities during one pulse the change in the donor concentration Ce^{3+} can no longer be approximated by a constant and the concentration of excited free electrons is large. This leads to a saturation of the refractive index that is proportional to $\Delta n \propto 1/\sqrt{(1+I)}$ (see (5)) in comparison to the saturation behavior at small intensities (see (4)) with $\Delta n \propto 1/(1+I)$ [20, 21]. The numerical integration of the wave equation (6) leads to an existence curve that fits very well to the experimental data (Fig. 5), supporting the idea that ps-solitons can be treated as high-intensity solitons.

The existence of solitons created with ultra short laser pulses depends on the overlap of the soliton pulse and the background pulse in time. On first sight it might look astonishing that the soliton and background pulse do not have to overlap in time to create a stable soliton. This can be understood in the framework of the light-induced charge transport in SBN. When the background pulse hits the crystal it excites electrons from Ce^{3+} ions to the conduction band. The lifetime of the electrons in the conduction band is on the order of several nanoseconds depending on the concentration of Ce^{4+} traps [24]. This means that the soliton pulse still experiences a background conductivity that has not been decreased to zero when the soliton pulse reaches the crystal. Hence, the value of the background photoconductivity at the time when the soliton pulse hits the crystal depends on the time delay between soliton pulse and background pulse. By comparing the existence curves for the different time delays one may deduce the order of the lifetime of excited electrons. Assuming a lifetime of about 4 ns will lead to a shift of the existence curves for the delayed pulses to smaller intensity ratios because the effective background intensity is a factor $\exp(-\tau_{delay}/\tau_e)$ smaller than the pulse intensity. The existence curves for the delayed pulses will shift to smaller intensity ratios when the effective background intensity is considered. This method of measuring the existence curve for different pulse delays can therefore be used to estimate the lifetime of excited electrons in photorefractive crystals. This method is not restricted to SBN, as it can be used for all photorefractive crystals where spatial screening solitons can be induced. For instance in $LiNbO_3$ crystals the lifetime of electrons is expected to be much smaller than in SBN crystals.

The formation of solitons with infrared light is possible as the infrared light can still excite electrons. Due to the smaller absorption of Ce^{3+} in the infrared the induced photoconductivity to screen the applied electrical field is also smaller but stable solitons can still be formed. The different quantitative behavior between the existence curves for visible and infrared light is not fully understood yet. Some material parameters like the electro-optic coefficient and the refractive index are smaller in comparison to the coefficients for visible light. It is most likely that the light-induced charge transport is different in the infrared spectral region and therefore the dependence of the nonlinearity on the light intensity is different. For example, two-photon absorption may play a major role at 800 nm for the excitation of electrons. Other impurities like antisite defects that can act as shallow traps can also contribute to the light-induced charge transport in SBN [24]. As solitons can be formed with picosecond laser pulses at 800 nm, it might be possible to create solitons with light in the telecommunication wavelength range since it has been reported that solitons can be formed at 1550 nm in planar SBN waveguides [27].

6 Conclusions

We have reported for the first time, to the best of our knowledge, on the formation of spatial optical photorefractive solitons with picosecond laser pulses. The dynamics and the existence curves for solitons created with laser pulses in the green wavelength region are very similar to the formation of solitons with cw-laser light. The main differences between

picosecond and cw solitons are the soliton widths at high light intensities and the existence range in dependence of the time delay between soliton pulse and background pulse. The differences can be explained by the light-induced charge transport in SBN with short laser pulses. The successful generation of solitons with ultra short infrared laser pulses gives the promising perspective to generate spatial solitons with light of the telecommunication wavelength range.

References

1. Y.S. Kivshar, G.P. Agrawal, *Optical Solitons: From Fibers to Photonic Crystals* (Academic Press, New York, 2003)
2. G.P. Agrawal, *Nonlinear Fiber Optics* (Academic Press, New York, 2006)
3. Y. Silberberg, Opt. Lett. **15**, 1282 (1990)
4. B. Malomed, D. Mihalache, F. Wise, L. Torner, J. Opt. B: Quantum Semiclass. Opt. **7**, R53 (2005)
5. X. Liu, L.J. Qian, F.W. Wise, Phys. Rev. Lett. **82**, 4631 (1999)
6. D. Mihalache, D. Mazilu, F. Lederer, Y.V. Kartashov, L.-C. Crasovan, L. Torner, Phys. Rev. E **70**, 055603 (2004)
7. D. Mihalache, D. Mazilu, F. Lederer, B.A. Malomed, Y.V. Kartashov, L.-C. Crasovan, L. Torner, Phys. Rev. Lett. **95**, 023902 (2005)
8. M. Segev, B. Crosignani, A. Yariv, B. Fischer, Phys. Rev. Lett. **68**, 923 (1992)
9. G.I. Stegeman, M. Segev, Science **286**, 1518 (1999)
10. M. Mitchell, Z. Chen, M. Shih, M. Segev, Phys. Rev. Lett. **77**, 490 (1996)
11. A.W. Snyder, D.J. Mitchell, Phys. Rev. Lett. **80**, 1422 (1998)
12. C. Weilnau, C. Denz, J. Opt. A: Pure Appl. Opt. **5**, 529 (2003)
13. T. Carmon, C. Anastassiou, S. Lan, D. Kip, Z. Musslimani, M. Segev, D.N. Christodoulides, Opt. Lett. **25**, 1113 (2000)
14. K. Motzek, A. Stepken, F. Kaiser, M.R. Belic, M. Ahles, C. Weilnau, C. Denz, Opt. Commun. **197**, 161 (2001)
15. C. Weilnau, C. Denz, M. Ahles, A. Stepken, K. Motzek, F. Kaiser, Phys. Rev. E **64**, 056601 (2001)
16. J. Petter, J. Schröder, D. Träger, C. Denz, Opt. Lett. **28**, 438 (2003)
17. W. Krolikowski, B. Luther-Davies, C. Denz, J. Petter, C. Weilnau, A. Stepken, M.R. Belic, Appl. Phys. B **68**, 975 (1999)
18. W. Krolikowski, C. Denz, A. Stepken, M. Saffman, B. Luther-Davies, Quantum Semiclass. Opt. **10**, 823 (1998)
19. C. Rotschild, B. Alfassi, M. Segev, O. Cohen, Nat. Phys. **2**, 769 (2006)
20. K. Kos, G. Salamo, M. Segev, Opt. Lett. **23**, 1001 (1998)
21. M. Segev, M.F. Shih, G.C. Valley, J. Opt. Soc. Am. B **13**, 706 (1996)
22. A.A. Zozulya, D.Z. Anderson, Phys. Rev. A **51**, 1520 (1995)
23. C. Denz, W. Krolikowski, J. Petter, C. Weilnau, T. Tschudi, M.R. Belic, F. Kaiser, A. Stepken, Phys. Rev. E **60**, 6222 (1999)
24. K. Buse, A. Gerwens, S. Wevering, E. Krätzig, J. Opt. Soc. Am. B **15**, 1674 (1998)
25. S. Wevering, K. Buse, S. Simon, R. Pankrath, E. Krätzig, Opt. Commun. **148**, 85 (1998)
26. A.A. Zozulya, D.Z. Anderson, A.V. Mamaev, M. Saffman, Phys. Rev. A **57**, 522 (1998)
27. M. Wesner, C. Herden, R. Pankrath, D. Kip, P. Moretti, Phys. Rev. E **64**, 036613 (2001)